DesignCon 2013

Impact of Probe Coupling on the Accuracy of Differential VNA Measurements

Sarah Paydavosi, Oracle Corp.
Laura Kocubinski, Oracle Corp.
Jason Miller, Oracle Corp.
Gustavo Blando, Oracle Corp.
Eugene R. Whitcomb, Oracle Corp.
Istvan Novak, Oracle Corp.

Abstract

Having an extremely stable and precise Vector Network Analyzer (VNA) measurement setup is imperative for the design validation, analysis and troubleshooting of package and printed circuit board (PCB) high-speed interconnects. In a four-port VNA configuration, differential measurements taken using ground-signal-signal-ground (GSSG) wafer probes include parasitic coupling between the probe tips that is not calibrated out using a manual short-open-load-thru (SOLT) calibration technique which employs a 12-term error model. This can result in measurement inaccuracy. In this paper, probe coupling and the consequent error on scattering parameters (S-parameters) will be measured and characterized as a function of spacing between the probes.

This uncompensated error can introduce inaccuracies in channel characterization, specifically far-end crosstalk, and may result in misleading conclusions. Defining the residual probe characteristics, besides probe-to-probe coupling, after an SOLT calibration will help to close the measurement-simulation correlation loop.

An approximate coupling model for differential probes will be developed, which will allow the possibility of modifying the VNA wafer-probe measurement results accordingly.

Author(s) Biography

Sarah Paydavosi is a hardware engineer at Oracle Corp. Her current work focuses on signal integrity modeling, analysis, and validation in Oracle's MicroElectronics ASIC and SoC IP group. She received her PhD in electrical engineering from Massachusetts Institute of Technology.

Laura J. Kocubinski is a hardware engineer at Oracle Corp. She currently works on signal integrity within Oracle's SPARC T-Series server division. She recently received her BSEE from Rensselaer Polytechnic Institute.

Jason R. Miller is a principal hardware engineer at Oracle Corp. where he works on ASIC development, ASIC packaging, interconnect modeling and characterization, and system simulation. He has published more than 40 technical articles on topics such as high-speed modeling and simulation, and he co-authored the book "Frequency Domain Characterization of Power Distribution Networks," published by Artech House. He received his PhD in electrical engineering from Columbia University.

Gustavo J. Blando is a principal hardware engineer with more than 10 years of experience in the industry. Currently at Oracle Corp., he is responsible for the development of processes and methodologies in the areas of broadband measurement, high-speed modeling, and system simulations. He received his MS degree from Northeastern University.

Eugene R. Whitcomb currently works as a hardware developer at Oracle Corp. with 40 years of industry experience. He received his associate’s degree in 1980 from NSCC in Electro-Mechanical Technology. He completed his bachelor’s degree and master’s degree in information technology from AIU in 2004 and 2006, respectively.

Istvan Novak is a senior principal engineer at Oracle Corp. Besides signal integrity design of high-speed serial and parallel buses, he is engaged in the design and characterization of power-distribution networks and packages for midrange servers. He creates simulation models and develops measurement techniques for power distribution. Novak has more than 20 years of experience with high-speed digital, RF, and analog circuit and system design. He has been made an IEEE fellow for his contributions to signal integrity and RF measurement and simulation methodologies.

1 Introduction

The VNA offers an extremely stable, precise, and versatile measurement platform for the design validation, analysis, and troubleshooting of package and PCB high-speed interconnects.

As electrical networks increasingly operate at higher frequencies, network analyzers are often employed to measure S-parameters. Characterizing electrical networks using S-parameters has gained popularity because signal power is easier to quantify than voltage or current at radio and microwave frequencies. The VNA utilizes ratios of power to define network characteristics, including, but not limited to, insertion loss and return loss.

Obtaining the best possible measurements with a VNA requires a solid understanding of the interaction between measurement components, possible sources of error, and error modeling. The accuracy of VNA measurements is determined by the accuracy and quality of calibration standards, the repeatability of the measurement systems, and the thoroughness of error models.

One significant challenge in VNA measurements is defining the reference plane, which is where the measurement system ends and the device under test (DUT) begins. With wafer probing, this boundary will often be located at the microwave probe tips. In a perfect world, with a perfect calibration, the system will measure only the characteristics of the DUT connected to the reference planes. In this paper, however, it will be shown that probe-to-probe parasitic coupling, as well as probe-to-DUT parasitics, may not be accounted for depending on the calibration routine and subsequent error terms. Specifically, in a four-port port VNA configuration, dual or differential wafer-probe-to-wafer-probe coupling is not accounted for in a standard 12-term error model SOLT calibration technique and can result in measurement error.

GSSG microwave probes are favorable for differential PCB measurements because of the conventional GSSG pad arrangement. Typical GSSG probes have signal tips that are arranged side-by-side; when carrying differential signals, the two tips create fringing fields. Such field patterns cause coupling between the tips [1]. We will show that this probe coupling is dependent on the DUT as well as the probe geometry.

When measuring differential PCB traces using wafer probes, the spacing between the tips of the GSSG probes is determined by the pitch of the measurement pads or traces. The spacing between the probe tips may need to be readjusted between measurements. Therefore, it is highly important to understand and quantify the possible measurement error caused by the coupling between probes.

In this paper, parasitic coupling between GSSG probes will be investigated and quantified. Several SOLT calibrations with different probe-to-probe spacings will be performed; measurements of different spacings applying the aforementioned calibrations will be taken. This will demonstrate that a manual SOLT calibration employing a 12-term error term model does not account for the effects of wafer probe coupling during VNA measurements.

Depending on the probe-to-probe spacing, far-end crosstalk measurements can vary up to 15 dB. Such variation between VNA measurements may raise valid concerns. Do differential wafer probe measurements reflect the true properties of the DUT or added error caused by probe-to-probe coupling?

Single-ended four-port port crosstalk measurements, which are often a serious consideration in PCB design, may be subjected to this inaccuracy.

By modeling the probe-to-probe coupling using several tools, we quantify the coupling as a function of distance. This will lend insight into the extent to which we can trust differential wafer probe measurements and the post-processing results.

2 The Calibration Process

Proper calibration of a VNA is necessary for accurate network measurements. A VNA calibration should define systematic errors that are mathematically removed during VNA measurements. Systematic errors are time-invariant measurement errors caused by the imperfections of the test setup and test equipment.

It is important to note that random errors, which are not accounted for during calibration, may be introduced during measurement. Such errors are non-repeatable and vary with time. Instrument noise, for example, may be defined as random error. Every VNA measurement is prone to measurement uncertainty, even with a "perfect" calibration.

One source of random error associated with our specific test setup was quantified in a simple study. This source of error is due to coaxial (coax) cable movement. The random error associated with coaxial cable movement was studied by taking measurements of a mechanical through (thru) with different cable orientations. Nine measurements of single-ended insertion loss of a measured mechanical thru are presented in Figure 1. Between measurements, the cables were placed in different orientations.

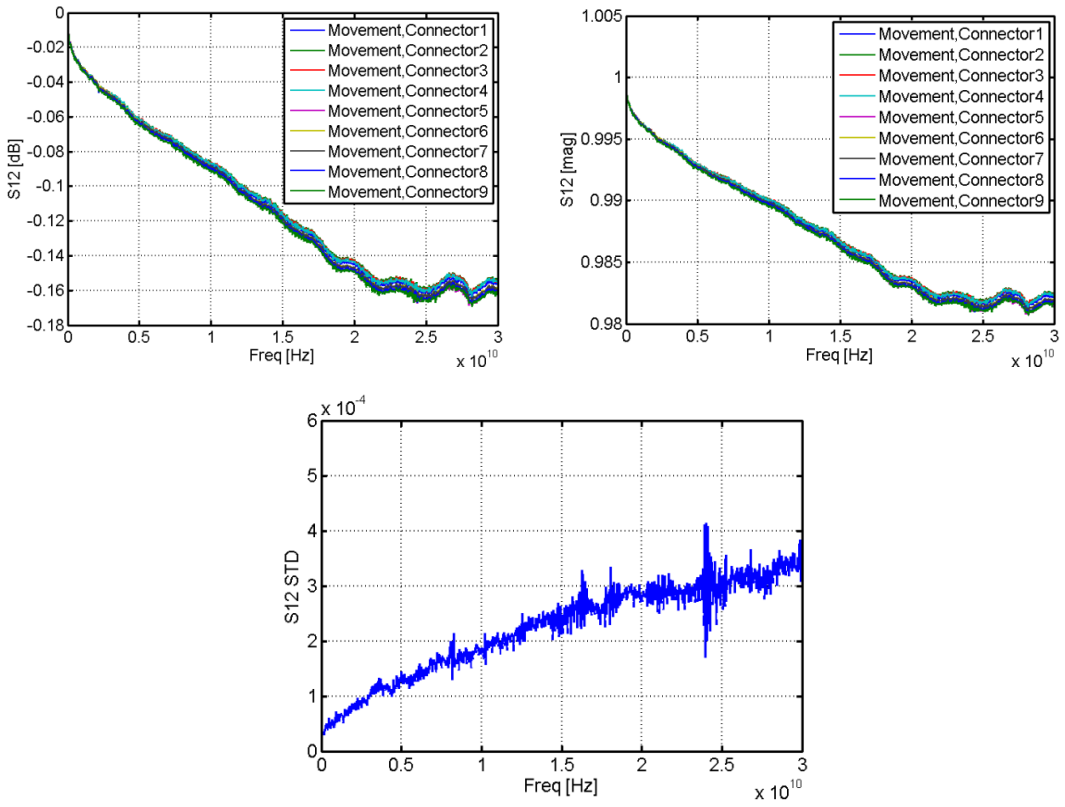

Figure 1 *Error associated with cable movement; (top left) Single-ended insertion loss of mechanical thru in decibels versus frequency; (top right) Single-ended insertion loss in magnitude versus frequency; (bottom) Standard deviation of single-ended insertion loss versus frequency*

It can be seen in Figure 1 that the greatest variation between measurements in decibels is in the range of 10e-2, at approximately 20 GHz. This amount of error gradually increases with frequency, but the cable

movement error in our measurement setup is still relatively small at all frequencies. The standard deviation plotted at discrete points is relatively small as well, with a peak value of 4.1455e-4, at approximately 25 GHz.

There are two common calibration methods: SOLT and Thru, Reflect, Line (TRL) calibration.

The SOLT calibration is perhaps the most common of all manual VNA calibration techniques. The SOLT calibration can be done with coaxial calibration kits or wafer probe calibration substrates. Figure 2 (a) shows a simplified calibration substrate with open, load and thru standards [2]. The calibration performed for the following measurements utilized a calibration substrate.

In an SOLT calibration, the reference plane of one probe is connected to each standard individually for the VNA to measure. After said measurements, the two reference planes are connected to form a thru as seen in Figure 2 (b).

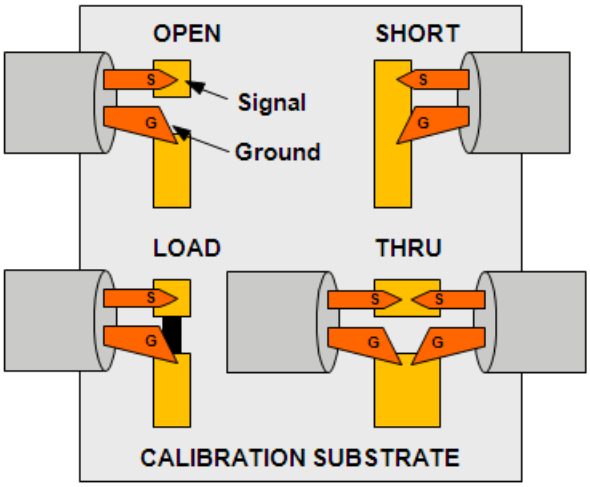

(a)

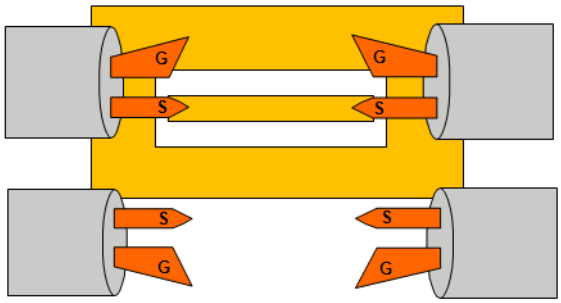

(b)

Figure 2 *(a) Simplified diagram of SOLT calibration substrate with short, open, load and thru standards; (b) Simplified calibration substrate loop-back thru standard, SOLT technique*

For a TRL calibration, the calibration standards can be fabricated and characterized using the same material as the DUT. For PCB applications, this means that some area of the PCB should be used for placing the calibration structures. In addition, well-constructed, repeatable standards are essential for the most accurate TRL calibrations.

Inhomogeneous dielectrics, PCB dimensional variations, and the glass-weave effect make it difficult to obtain accurate measurements using the TRL method. Expanding upon this point, the glass-weave of the laminate may not run parallel relative the traces, as illustrated in Figure 3 [3].

Figure 3 *Photograph of glass-weave with two differential pairs (arrows are aligned with the two differential pairs and a portion of the upper pair is highlighted in red); the angle of the weave relative to the trace is apparent and several horizontal glass bundles are highlighted in black*

In fact, the glass-weave routing angle may not be consistent throughout the length of differential net. This is just one of many possible asymmetries that could introduce error into a TRL calibration.

The study of calibration methods other than SOLT is outside of the scope of this paper. The manual SOLT calibration was used for calibration of the measurement system up to the tips of the differential probes unless otherwise noted.

The four-port port SOLT calibration used for the following measurements utilizes a 12-term error model. These error terms correct for the inaccuracies of coupler directivity, source match, load match, reflection tracking, transmission tracking, and internal receivers crosstalk (leakage) [4]. However, the 12-term error model used to correct the measurements cannot mathematically correct for coupling at the reference planes [1] [5] [6].

There are calibration methods that include 16-term error models that include leakage at the test ports and reference planes, but such calibrations mostly require specific or custom calibration substrates and have not been implemented in most VNAs.

The effect of coupling between probes on calibration accuracy and measurement results will be studied in the following sections.

3 Coupling Observed During Measurement

In order to study the effect of probe-to-probe coupling, several calibrations were performed using 500 µm pitch differential wafer probes. Manual SOLT calibrations were performed with 280 µm, 450 µm, and 2000 µm spacing between the probes tips. After the calibration of the measurement system, the two differential probes were touched in the air, effectively creating a thru, as seen in Figure 4 below. Measurements were then taken at constant probe spacing while applying the different calibrations.

It is assumed that at a spacing of 2000 µm there is minimal or negligible probe-to-probe crosstalk.

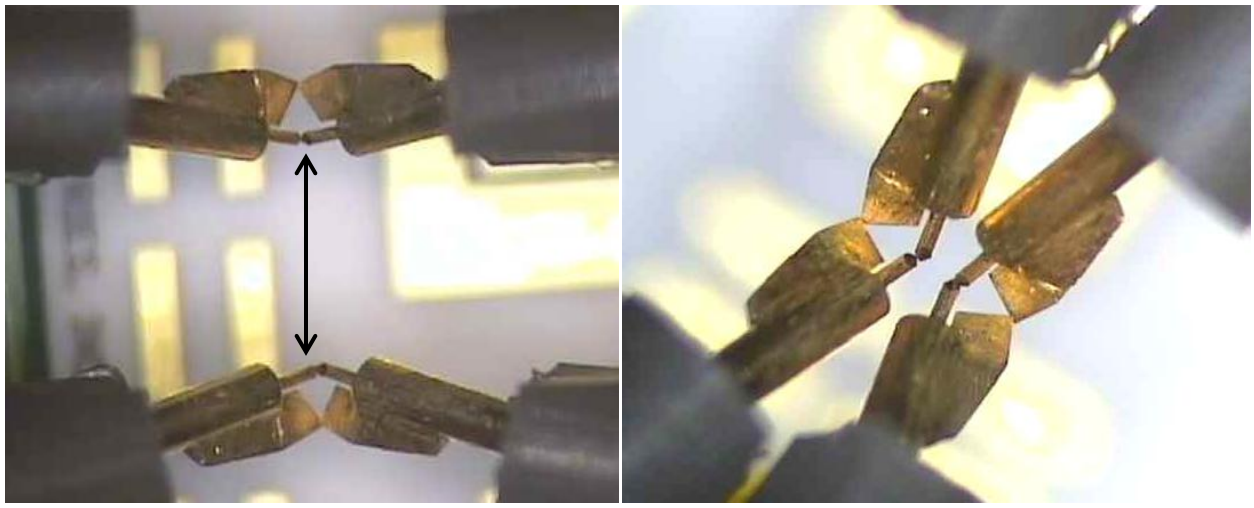

Figure 4 *Studying the coupling between GSSG wafer probes by touching them in air and performing a thru measurement at different spacings; (left) 2000 µm spacing; (right) 450 µm spacing*

Near-end crosstalk (NEXT) and far-end crosstalk (FEXT) measurements are shown in Figure 6 and Figure 7 below. All the S-parameters presented have been normalized to 50 ohms. The port assignments can be seen Figure 5.

Figure 5 *Port assignments to be used for the interpretation of the S-parameters presented*

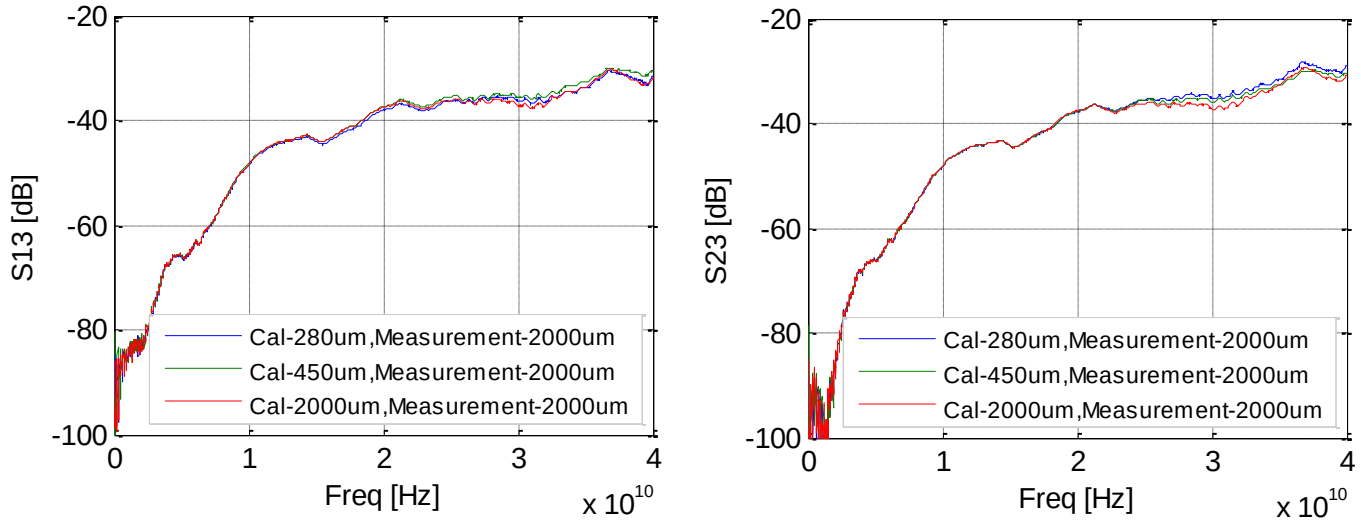

Figure 6 *S-parameters measured via VNA while probes touching thru in air with 2000 µm spacing and the 3 aforementioned SOLT calibrations applied; (left) S13; (right) S32*

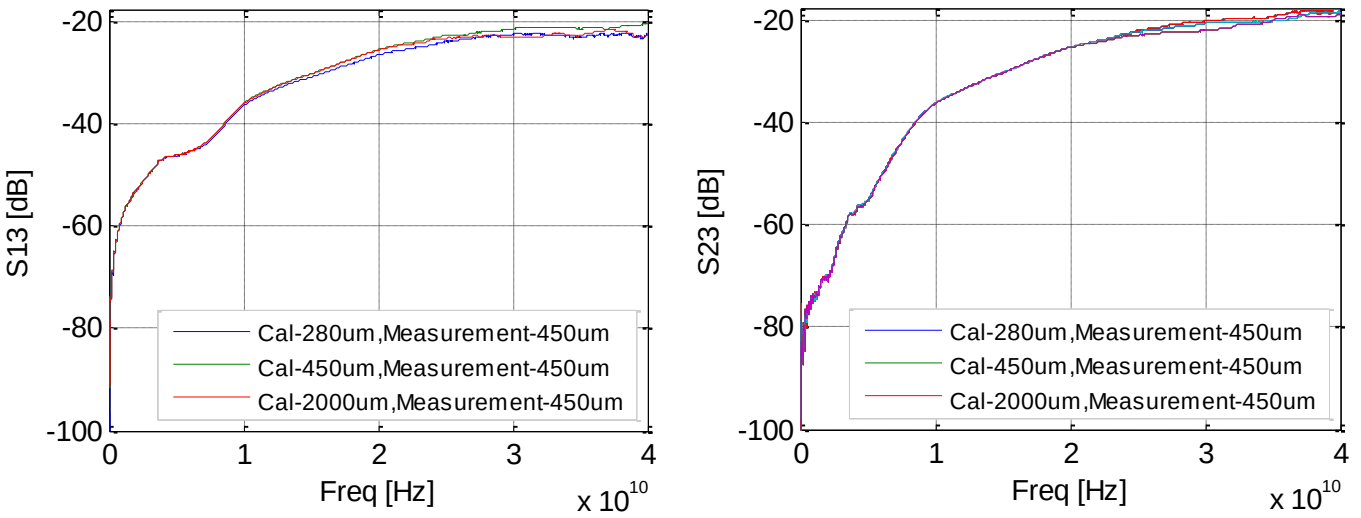

Figure 7 *S-parameters measured via VNA while probes touching thru in air with 450 µm spacing and the 3 aforementioned SOLT calibrations applied; (left) S13; (right) S32*

When the probes were positioned thru in the air with a spacing of 2000 µm and 450 µm and the calibrations performed at different spacings (450 µm, 500 µm, and 2000 µm) were applied to the measurement, minimal change in probe-to-probe crosstalk is observed. This might suggest that coupling is not being captured during calibration.

This possible failure to account for probe-to-probe coupling in calibration was further studied by calibrating the measurement system only to the end of the coaxial cables (redefining the reference planes) using an electronic calibration (eCal) module and similarly measuring the probes touching in the air [7]. The measurements corrected with an electronic calibration should contain the characteristics of the probes, as the reference plane has been redefined.

Figure 8 below shows the NEXT for probe spacings of 280 µm, 450 µm, and 2000 µm. For each measurement, eCal was applied to the measurement as well as the SOLT calibration. This figure shows the measurements corrected with the electronic calibration juxtaposed with measurements corrected with the SOLT calibration.

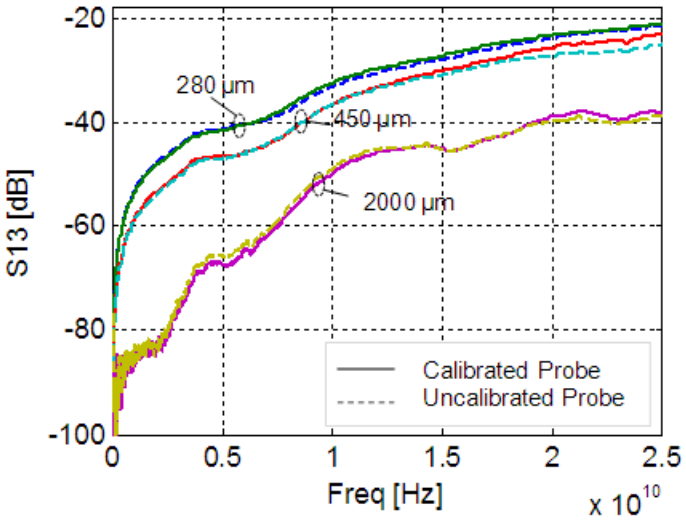

Figure 8 *The comparison of S13 measured with two different calibration methods, eCal and SOLT, via calibration substrate, at 3 different spacings*

As is shown in Figure 8 above, the crosstalk (S13) is defined similarly whether the calibration is done up to the end of the coax cables (eCal) or the probe tips (SOLT). This suggests that when performing an SOLT calibration, the coupling between the probes is not de-embedded from the measurement.

Regardless of the probe spacing during an SOLT calibration, the probe-to-probe coupling will affect the measurement result, which is dependent on the probe tip-to-tip spacing. This can be seen in the above figure and will be characterized in the following sections.

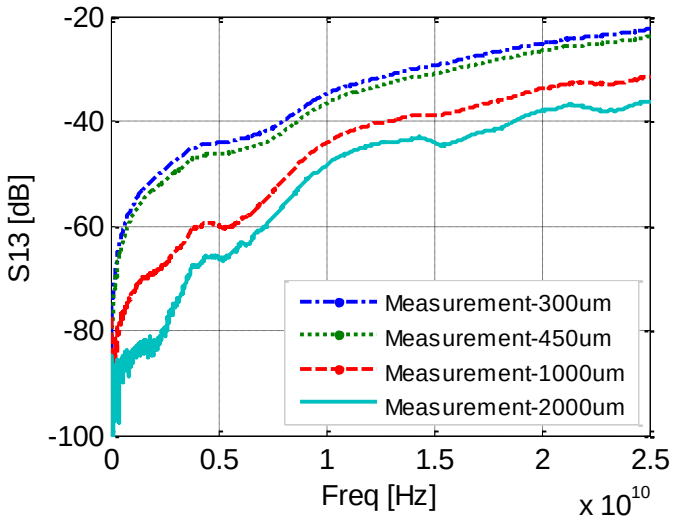

Figure 9 *S13 measured while applying the SOLT calibration (performed with a probe spacing of 280 µm) with probe-to-probe spacing of 300 µm, 450 µm, 1000 µm, and 2000 µm*

In Figure 9 above, it can be inferred that probe-to-probe crosstalk is a function of distance between probe tips. As one might expect, more crosstalk is measured as the probes are spaced closer to one another. For this probe-to-probe configuration, the difference between single-ended crosstalk for different probe-to-probe spacings is nearly 15 dB.

It should be noted that at lower frequencies, the measured crosstalk is so small (-60 dB or lower) that this measurement is too close to the noise floor of the VNA and thus outside of the instrument's accuracy range.

4 Measurement and Simulation Correlation

4.1 3D Field Solver Probe Thru Model

A 3D field solver was used to perform full-wave field simulations using the reference [8]. Since the details of the probe construction were unavailable, the probe geometry and dimensions were measured under a microscope; a three-dimensional structure was manually created including the coax sleeve, ground blade, and the center pin. The coax dielectric material was approximated as Teflon, and the conductors were assigned as copper. Four waveports were used at the end of the coax, and a radiation boundary was applied to the surrounding airbox. The project was parameterized so that different signal-to-signal spacings could be simulated.

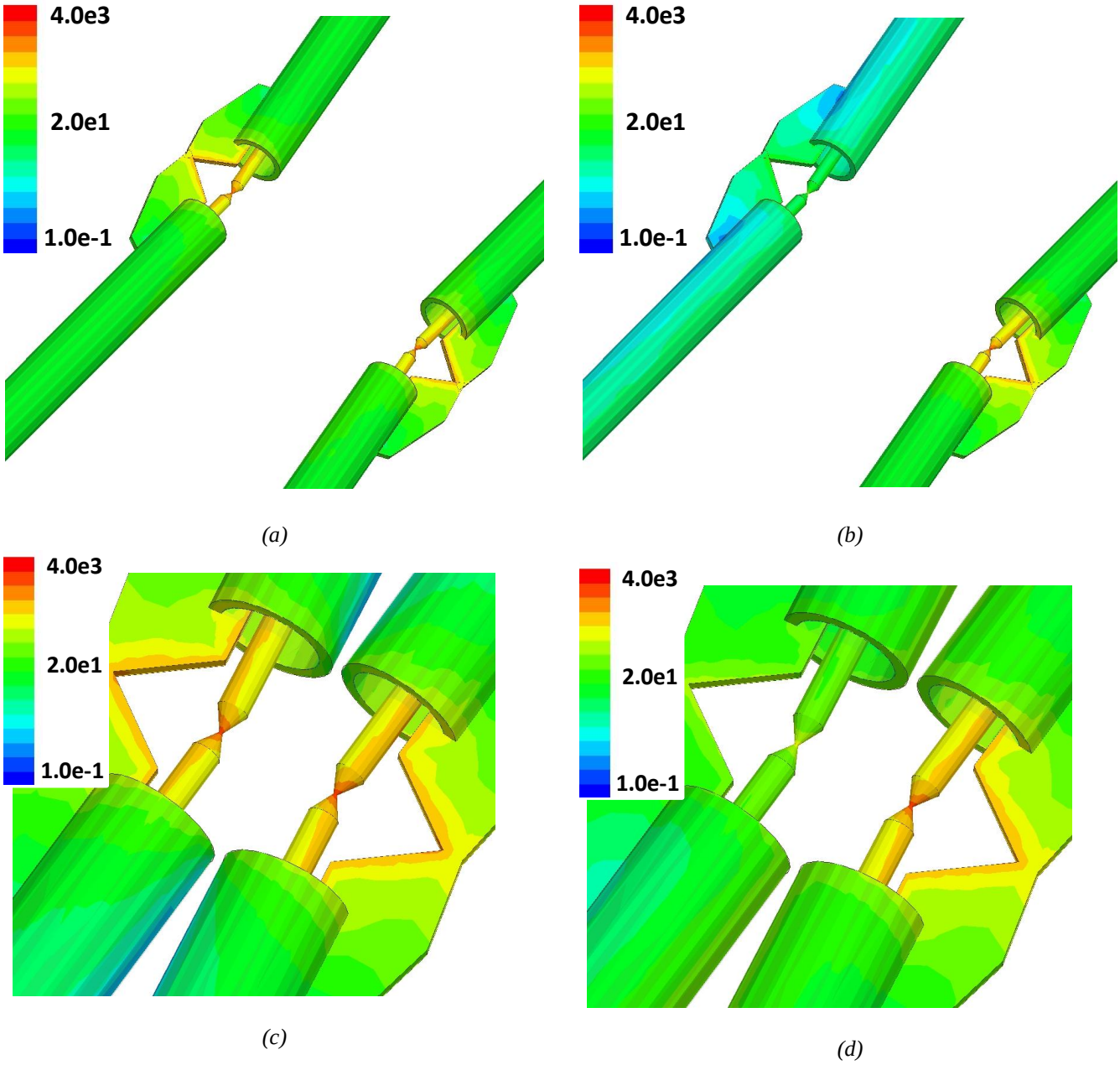

Figure 10 *3D simulation of 500 µm pitch differential wafer probes; (a) Two probes excited with 2000 µm spacing; (b) One probe excited with 2000 µm spacing; (c) Two probes excited with 450 µm spacing; (d) One probe excited with 450 µm spacing*

The current density plots shown in Figure 10 were created using two different port assignments. In the first assignment, each probe was excited equally and in phase. This allows us to visualize the current flow on each probe and the return current on the ground blade. In the second assignment, only one probe was excited. By doing this we can see the coupled current to the neighboring probe, which is almost ten times higher for the case with smaller probe spacing at the frequency of 20 GHz.

The S-parameters extracted from the 3D simulation are shown in Figure 11. In this figure, insertion loss, reflection loss, near-end crosstalk, and far-end crosstalk are plotted versus the thru probe measurement when the system was calibrated to the end of the coaxial cables (eCal).

Differences between simulation results and measurements may be attributed to the coaxial connectors (which were not included in the simulation); the probe-to-probe contact area formed when probes from opposite sides are touching; and the material and dimensional properties of the probes, which were estimated.

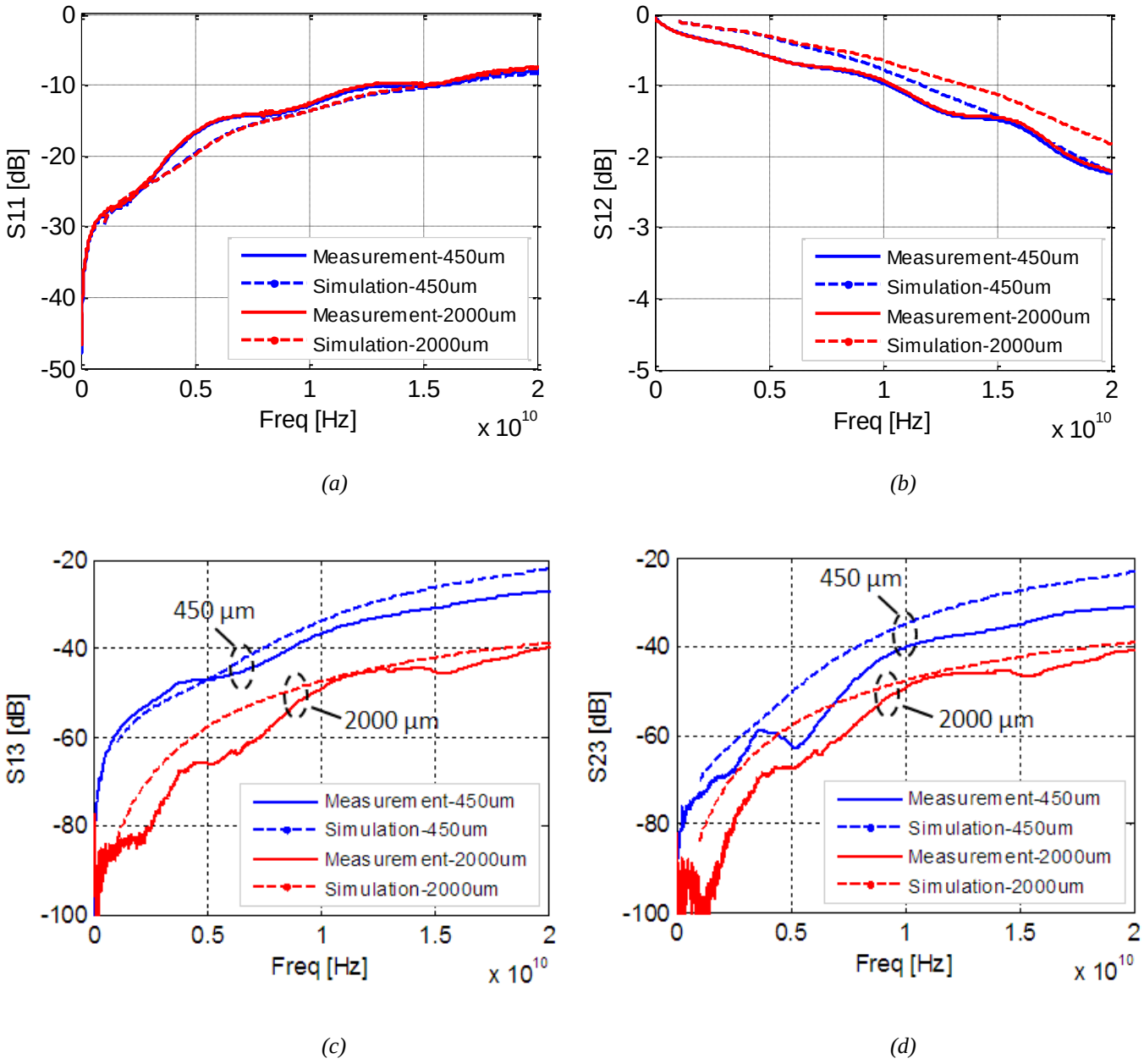

Figure 11 *3D simulation versus measurement results of two differential probes touching with 2000 µm and 450 µm spacing between probes; (a) Insertion loss; (b) Reflection loss; (c) NEXT; (d) FEXT*

4.2 Equivalent Circuit Thru Probe Model

In order to quantify the thru probe-to-probe coupling, an equivalent circuit model for the touching probes was created using [9]. Said circuit model can be seen in Figure 12 below.

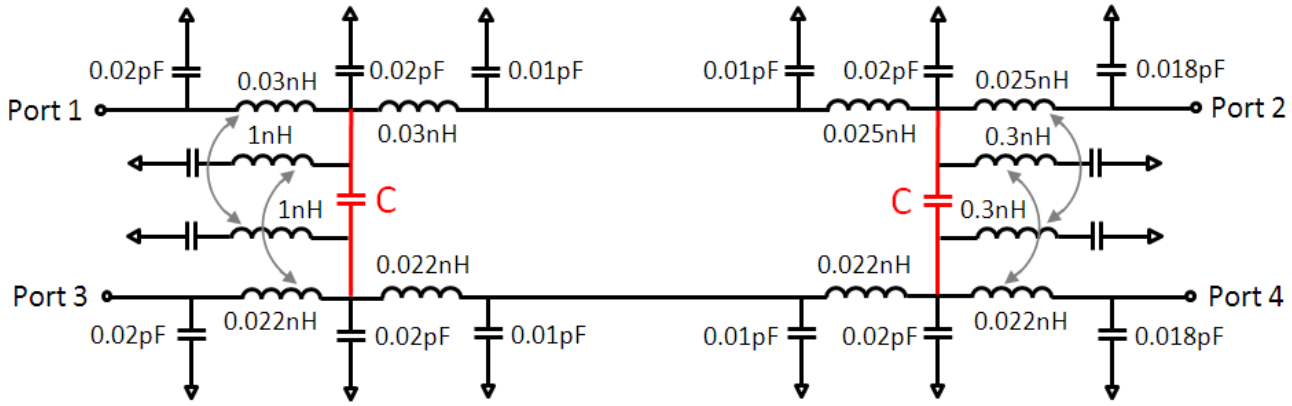

Figure 12 *Equivalent circuit model of thru probes touching with inductive and capacitive coupling; capacitive coupling between probe tips is highlighted in red, and inductive coupling is highlighted in gray*

Each individual probe was modeled with circuit elements as a series inductor and shunt capacitor in a pi configuration. The capacitive coupling between the signal pins was modeled by adding a capacitor between two the probes tips. Both inductive and capacitive coupling were needed in order to get a good fit to the measurement data while the probe spacing was 2000 µm. The inductive coupling was modeled by adding a series capacitor and inductor to each probe with mutual inductance between the mentioned inductor with the other probe. Adding this series inductor and capacitor helps by adding more poles to the model and consequently achieves better match at low frequencies.

It is shown in Figure 13 that probe-to-probe coupling can be captured by changing just the value of the coupling capacitor. It should be noted that this probe model was generated based on the calibrated probes and is mainly capturing the probe characteristics that have not been de-embedded during calibration.

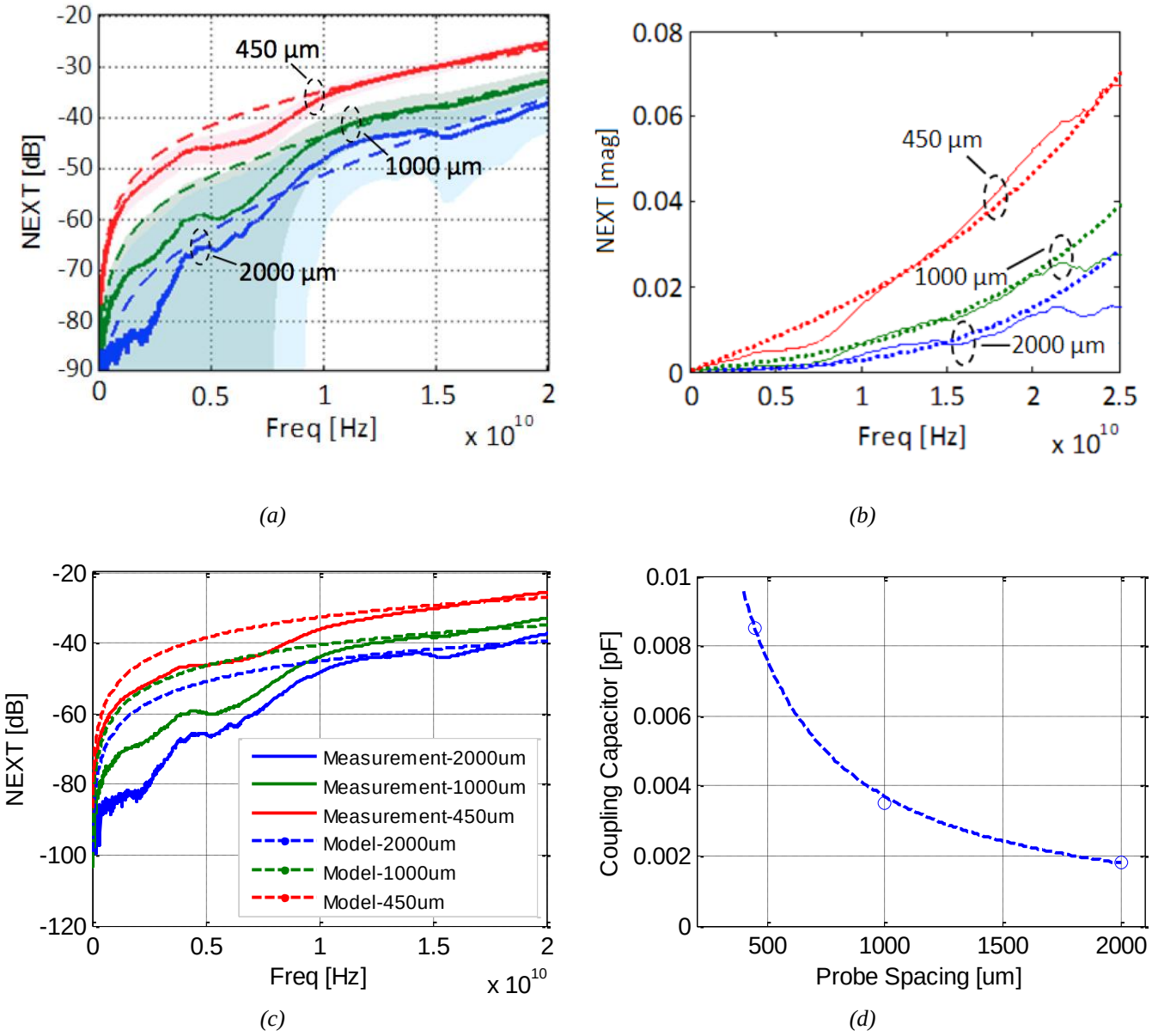

Figure 13 *(a) Near-end crosstalk of equivalent circuit model with inductive and capacitive coupling versus measurement for three different probe spacings; error bands represent the VNA measurement system inaccuracy; (b) Near-end crosstalk in magnitude of equivalent circuit model with inductive and capacitive coupling; (c) Near-end crosstalk of simplified (only capacitive coupling) equivalent circuit model versus measurement for three different probe spacings; the model fits the near-end crosstalk well above 10 GHz; (d) Coupling capacitance as a function of spacing between probe tips for the simplified probe model*

As mentioned, at low frequencies the amount of the crosstalk is so small that it is not within the accuracy range of the VNA. VNA measurement accuracy has been characterized in a separate internal study by repeating the measurement and probe landing, performing several calibrations, and moving the cables between each measurement. A part of this error study was presented earlier in the paper. The error bands associated with these sources of error are depicted in Figure 13 (a).

Since the amount of coupling is relatively small for frequencies less than 10 GHz and capacitive coupling is mostly dominant, we can neglect the inductive coupling, as is displayed in the model in Figure 16 (b). A simplified model with only capacitive coupling was used for the remaining simulations presented in the paper.

For each spacing, the value of the coupling capacitor is adjusted to get the best fit to the measurement data. The value of the coupling capacitor in picofarads decreases exponentially by increasing the probe spacing in microns. The value of the coupling capacitor follows the equation

$$C_{coupling}(x) = \alpha x^{-\beta}$$

where $\alpha = 4.87$, $\beta = 1.04$, x is in microns and C is in picofarads.

4.3 Separated Probe Model

To study the effects of probe-to-probe coupling on a real world DUT, wafer probe VNA measurements were taken on a differential net with the 500 μm pitch GSSG wafer probes. This net was a straight, isolated 2.428" stripline in a practical PCB. In order to land the differential probes on the stripline, a small section of trace was exposed and ground was connected from upper and lower layers, as can be seen in Figure 14. The width of each copper trace was approximately 6 mils (152.4 μm). The spacing between the traces was approximately 6 mils as well. The measurement was taken with a probe-to-probe spacing of approximately 400 μm.

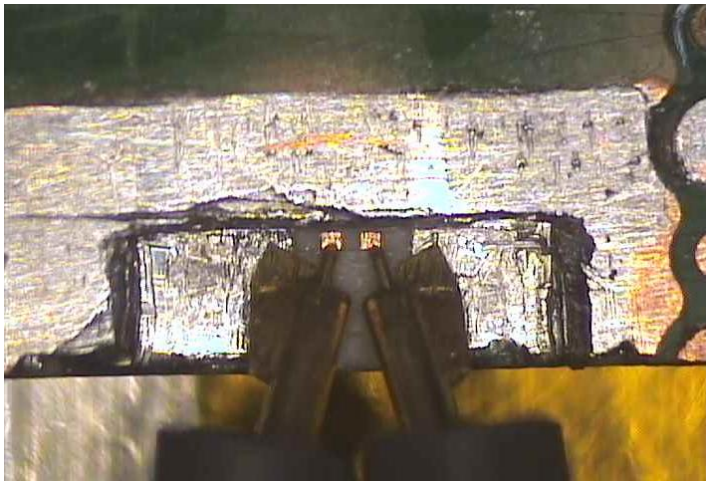

Figure 14 *500 μm pitch wafer probes landed on an exposed stripline in order to study the effects of probe-to-probe coupling on a practical DUT*

The measured S-parameters of the straight differential stripline were correlated to a 2D simulated differential transmission line model using reference [10], as seen in Figure 15.

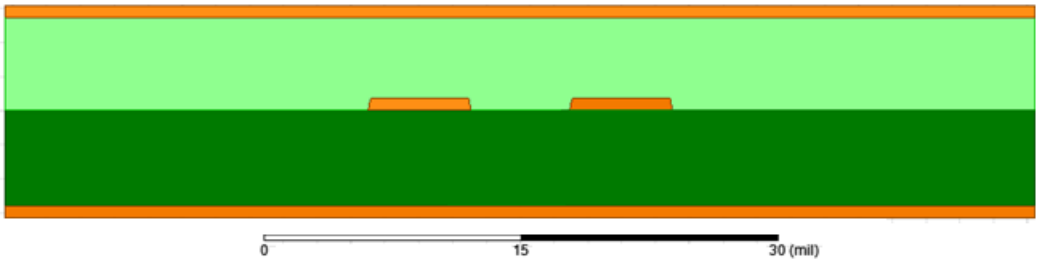

Figure 15 *Front view of differential stripline model used to correlate with measured S-parameters via VNA*

The S-parameters of the 2D simulated model were then cascaded with the separated probe model; the "complete" probe-DUT-probe model follows the diagrams and equivalent circuit presented in Figure 16.

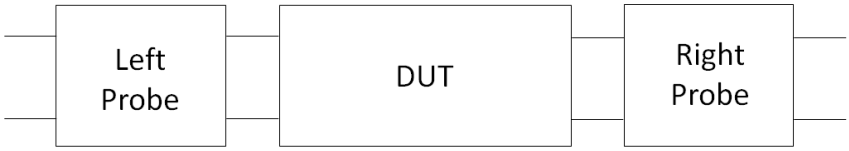

(a)

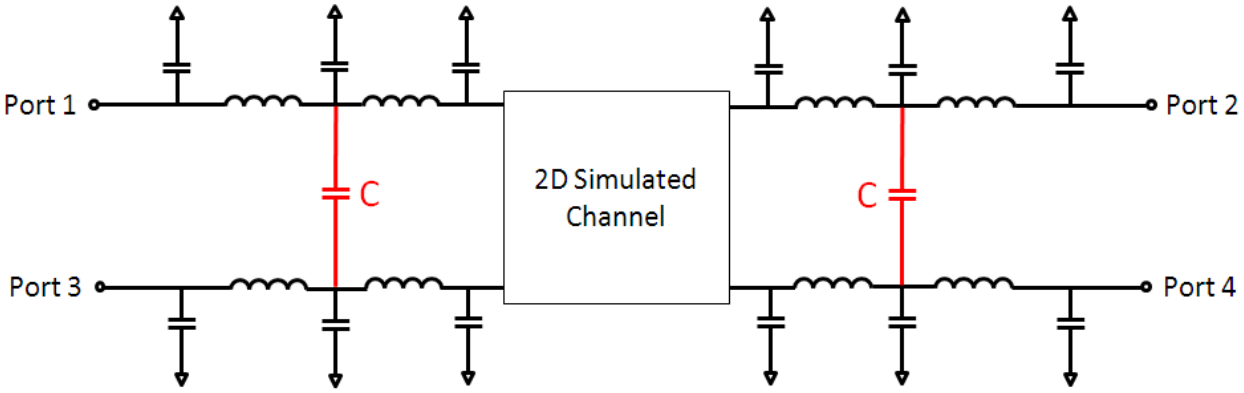

(b)

Figure 16 *(a) Block diagram of probe model cascaded with DUT; (b) Complete model of probe-DUT-probe with coupling capacitor highlighted in red*

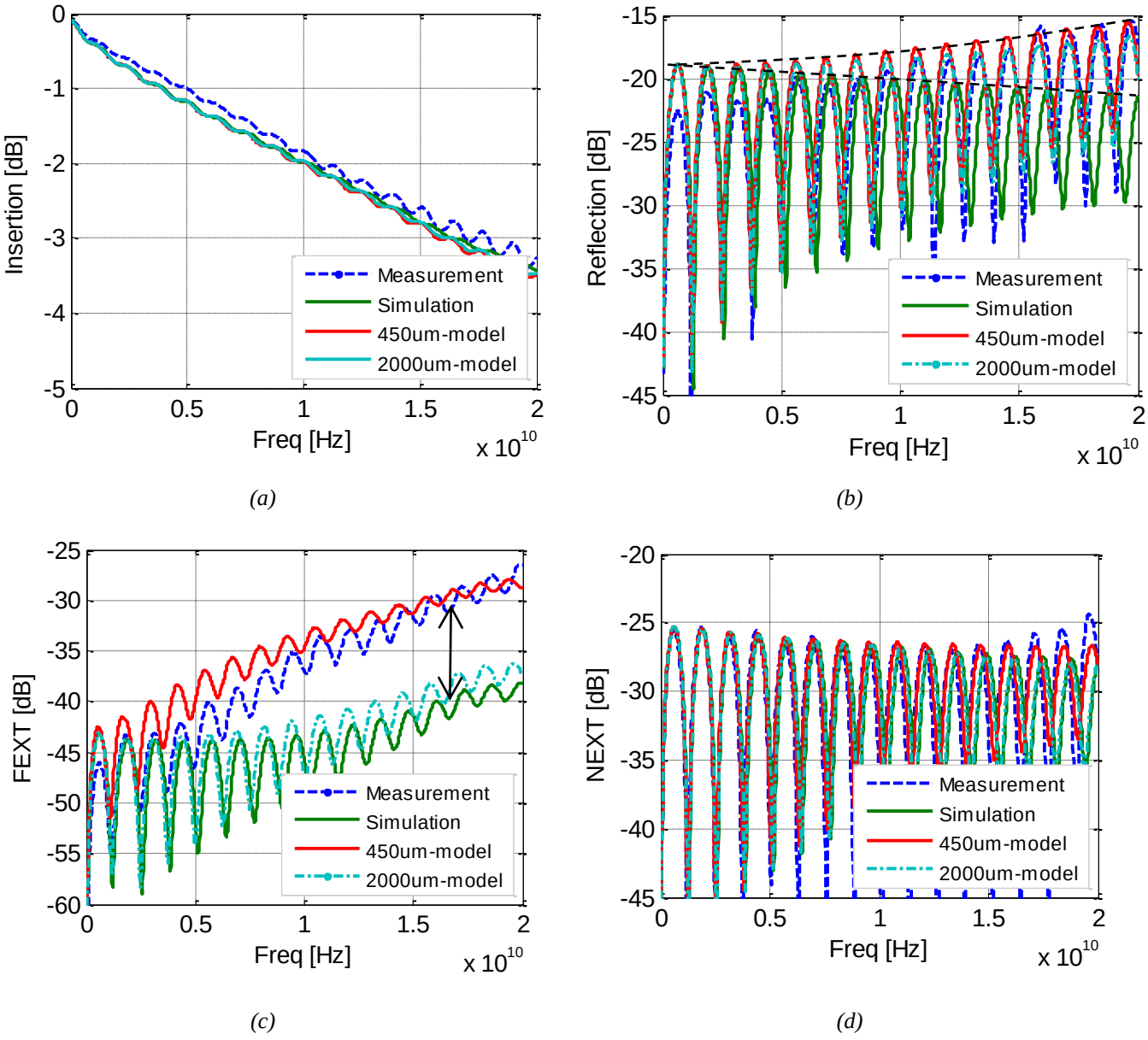

Figure 17 *Juxtaposed S-parameters from wafer probe VNA measurement, correlated 2D simulation of measured differential net, and complete 2D simulation with probe model at the beginning and end of DUT; (a) Single-ended insertion loss; (b) Single-ended return loss; (c) Single-ended near far-end crosstalk; (d) Single-ended near-end crosstalk*

Figure 17 shows that even after an SOLT calibration, there remain inductance and capacitance due to the GSSG probes that are not calibrated out and present in the S-parameters. It can be seen that in the ideal 2D simulation without probes, the single-ended return loss stays relatively flat up to 40 GHz.

In the VNA wafer probe measurement and the probe-DUT-probe model, the probe parasitic capacitance and inductance manifest as an upward slope with increasing frequency in single-ended return loss. With

different probe-to-probe spacing, simulated by changing the value of the coupling capacitor, single-ended insertion loss, return loss, and near-end crosstalk do not vary significantly.

However, looking at the probe-to-probe impact on FEXT is interesting. With a probe-to-probe spacing of 2000 μm, where the probe coupling is assumed to be negligible, the probe-DUT-probe simulation matches the 2D stripline simulation without probes relatively well. The probe-DUT-probe model, where the spacing between probes is 450 μm, matches the wafer probe VNA measurement where the probe-to-probe spacing was 400 μm. This suggests the probe coupling is the source of mismatch between simulated and measured FEXT.

It is logical that FEXT is noticeably affected by probe-to-probe coupling while probe-to-probe coupling affects NEXT negligibly. For NEXT crosstalk, the relative amount of coupling between differential traces masks the smaller amount of probe-to-probe coupling in a homogeneous stripline; this can be observed in Figure 18. The constant velocity in a homogeneous media (such as a stripline) forces far-end crosstalk noise to be small. As a result, the effect of probe coupling is more obvious for far-end crosstalk by adding inhomogeneous probes.

The effects of probe-to-probe coupling on near-end crosstalk and far-end crosstalk versus trace spacing and probe spacing are depicted in Figure 18.

Although the impact of probe characteristics on the measurement results (insertion loss, near-end crosstalk) may be small, in scenarios where accuracy matters, it is important to understand and quantify the probe-to-probe and probe-to-DUT interaction, as de-embedding these characteristics helps to uncover the characteristics of the DUT itself. It becomes clear that in any GSSG probe measurement, there is a certain amount of unavoidable error caused by the electromagnetic interaction between probes and DUT that is evident in single-ended return loss.

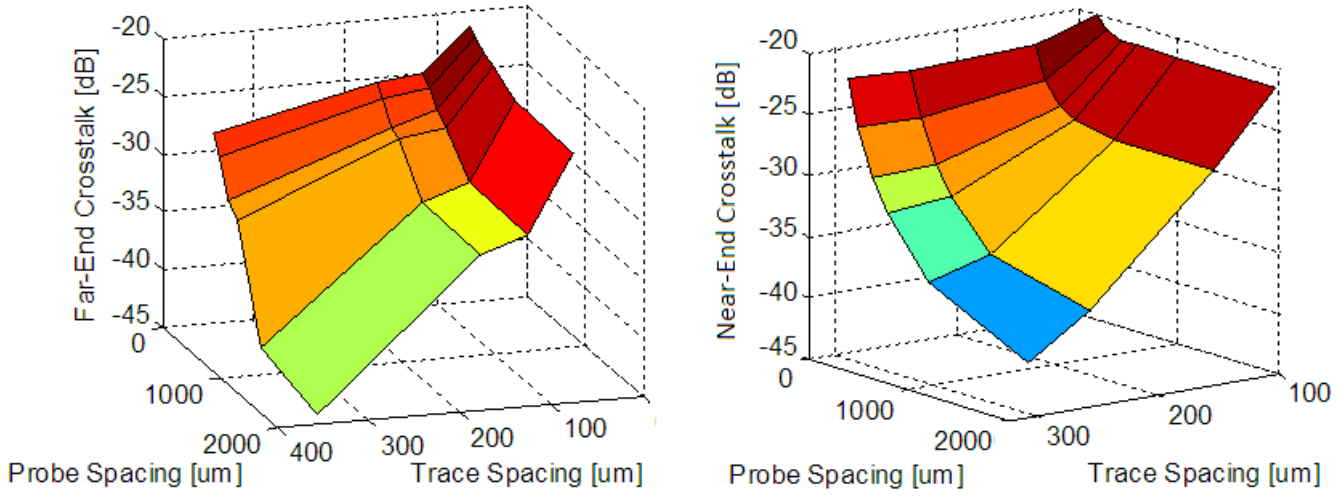

(a) *(b)*

Figure 18 *(a) Far-end crosstalk as a function of trace spacing and probe spacing; (b) Near-end crosstalk as a function of trace spacing and probe spacing*

As shown in Figure 18 (b), for highly coupled traces, NEXT does not change significantly as a result of probe coupling. However, the effect of probe coupling can be noticeable for loosely coupled traces.

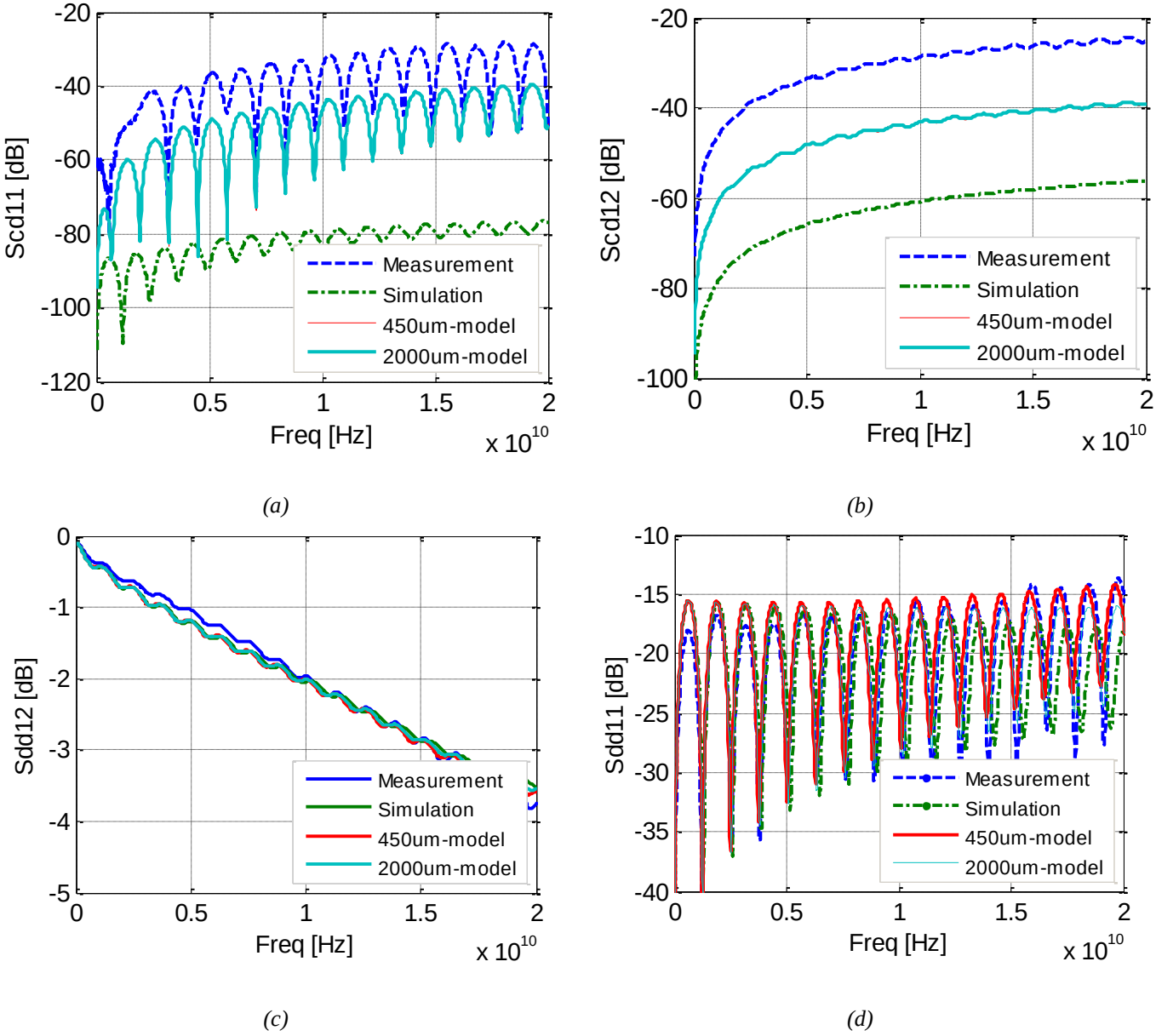

Figure 19 *Mixed-mode S-parameters of wafer probe VNA measurement, correlated 2D simulation of measured differential net, and complete 2D simulation with probe model at the beginning and end of DUT; (a) Differential to common reflection; (b) Differential to common insertion; (c) Differential insertion; (d) Differential reflection*

The near-end differential to common conversion is calculated as

$$Scd11=(S11+S31-S13-S33)/2$$

However, the ideal, symmetric transmission line model generated by the 2D simulator does not capture the measured mode conversion as shown in Figure 19. This mode conversion can be a result of reflection difference at port 1 and 3, or near-end crosstalk, between these two ports. Since the 2D model is close to symmetric, mode conversion is not affected by changing the spacing between the probes. The asymmetry of the probes which is captured in the equivalent circuit model is the source of the observed mode conversion in Figure 19.

The differential to common-mode transmission at ports 1 and 3, which is calculated as

$$Scd21=(S21+S41-S23-S43)/2$$

suggests that in addition to the probes, the difference or asymmetry of the two measured differential traces might also responsible for the observed difference between the measurement and simulation.

Asymmetry in the measured differential stripline may be attributed to non-uniform dielectric. The glass-weave in the dielectric may cause P and N asymmetries that become apparent in skew between traces, different trace impedances, differences in single-ended insertion loss, mode conversion, etc.

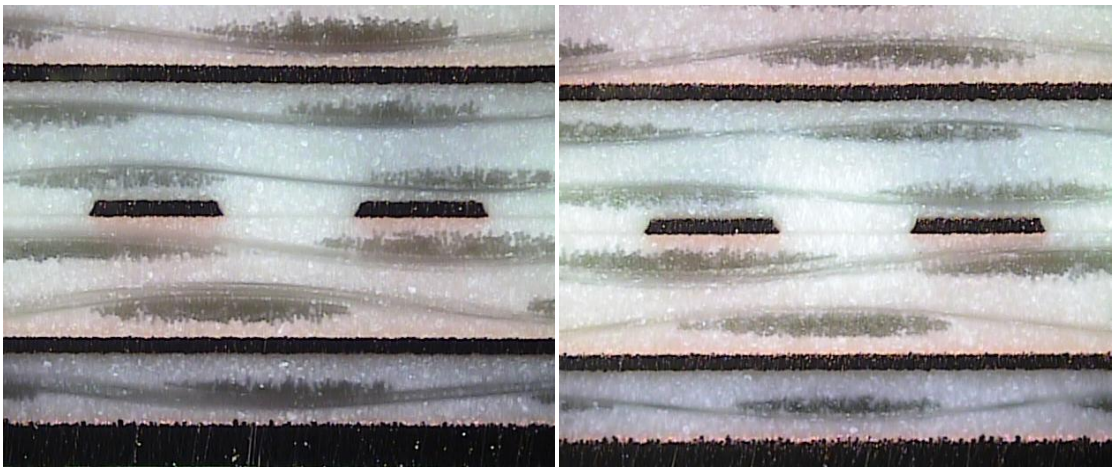

Figure 20 *Cross section of the stripline measured with the wafer probes and correlated to 2D simulation at two different locations; the black areas are the copper traces and ground planes, the light areas are the resin and the dark areas are the glass bundles (glass weaving)*

Figure 20 shows the glass bundles at two different two locations along the test board. It should also be noted that the glass bundles do not remain in a constant location; this suggests that the glass-weave is oriented at an angle relative to the different net, as mentioned earlier. This weaving effect may create a non-uniform dielectric constant since the dielectric of glass is much higher than that of epoxy.

5 Summary/Conclusion

Modeling the residual capacitive and inductive characteristics of GSSG probes unaccounted for in an SOLT calibration with a 12-term error model is useful for understanding the impact of wafer probes on VNA measurements. Including the probe characteristics in simulations will help to close long standing wafer probe measurement and simulation discrepancies. The variation of FEXT and return loss between different wafer probe measurements may now be explained as we close the measurement-simulation correlation loop. The proposed methods for modeling probes may be used to de-embed the probe characteristics from measurements, revealing the true characteristics of the DUT. More specifically, measurements may be taken with calibrated probes (up to coaxial cables) and during post-processing, the probe characteristics may be de-embedded using a 3D probe model, which would effectively leave the properties of just the DUT in the measurements.

The residual GSSG probe characteristics manifest as an upward slope in the return loss. If the characteristics of the probes are not de-embedded from the measurements, measured single-ended return loss may surpass a mask, when in the reality, the mask has not been broken.

The observed probe-to-probe coupling in the measurement and simulations studied mostly affects far-end crosstalk. No significant impact on simulated eye diagrams was observed.

SOLT calibration is a desirable calibration technique for PCB VNA wafer measurements considering the possible errors associated with a TRL calibration method due to geometry variation and inhomogenous materials of the customized calibration standards. It may be of interest to modify the 12-term error model used for an SOLT calibration to account for probe coupling as well as residual probe-DUT parasitics.

6 Acknowledgments

The authors would like to thank OJ Danzy and Mike Resso for their recommendations and ideas. The authors would also like to thank GCE and Joe Beers for the cross sectioning of the test board as well as William Coulliard for the machine tool work for the test board.

7 References

[1] Cascade Microtech Inc., “Making Accurate and Reliable 4-Port On-Wafer Measurements,” Application Note, 2009.
[2] Howard Heck, “Advanced Transmission Lines; 2 Port Networks & S-Parameters,” OGI EE564.
[3] Jason R. Miller, Gustavo J. Blando, Istvan Novak, “Additional Trace Losses due to Glass-Weave Periodic Loading,” DesignCon 2010, Santa Clara, CA.
[4] Roger B. Marks, “Formulation of the Vector Network Analyzer Error Model including Switching Terms,” ARFTG Conference Digest-Fall, 50th, Vol.32, No., pp.115-126, Dec. 1997.
[5] Agilent Technologies, “On-Wafer Vector Network Analyzer Calibration and Measurements,” Application Note.’
[6] Doug Rytting, “Network Analyzer Error Models and Calibration Methods,” Agilent Technologies.

[7] Agilent Technologies, Microwave Two-Port Electronic Calibration Module N4692-60003, Reference Guide, http://www.agilent.com
[8] Ansoft HFSS Version 9.2.1, from Ansoft Corporation.
[9] Advanced Design System Version 2011.10, from Agilent Technologies.
[10] Ansoft Q3D Extractor Version 11.0 from Ansys Inc.
[11] Agilent Technologies, "Applying Error Correction to Network Analyzer Measurements," Application Note 1287-3, March 27, 2002.
[12] D. F. Williams, J. C. M. Wang, and U. Arz, "An Optimal Vector-Network-Analyzer Calibration Algorithm," IEEE Transactions on Microwave Theory and Techniques, Vol. 51, No. 12, Dec. 2003.
[13] L. Hayden, "A Hybrid Probe-Tip Calibration for Multiport Vector Network Analyzers," IEEE 68th ARFTG, Dec. 2006.
[14] T. Lesher, L. Hayden, "A High Isolation Dual Signal Probe Technology," ARFTG, Dec. 2004.